ACS APPLIED MATERIALS & INTERFACES

Research Article

www.acsami.org

Luminescence Enhancement after Adding Organic Salts to Nanohybrid under Aqueous Condition

Daqing Yang, Yige Wang, Yu Wang, Zhiqiang Li, and Huanrong Li*

School of Chemical Engineering and Technology, Hebei University of Technology, GuangRong Dao 8, Hongqiao District, Tianjin 300130, China

Supporting Information

ABSTRACT: Lanthanide-based organic−inorganic hybrid materials (LnOIH) are of immense importance for various applications nowadays, while it still remains a significant challenge to achieve high luminescence efficiency in aqueous environment. Herein we present a simple and environmentally friendly two-step strategy to prepare strongly red-light emitting nano-LnOIH by first in situ forming Eu^{3+}-β-dikeonate complexes on Laponite platelets and subsequently increasing the coordination number of the complexes via the modification with a silane-functionalized imidazolium salt, which can fully protect Eu^{3+} ions from the water molecule quenching. The mechanism of how the imidazolium salt favors the formation of Eu^{3+}-β-dikeonate complex with large coordination number was elucidated. The result is that the removal of the abundant protons on the Laponite platelets through a mechanism of synergic effect of ion exchange and neutralization drives the formation of Eu^{3+}-β-diketonate complexes with high coordination number. The high efficiency of the resulting luminescent nano-LnOIH in water endows the nanohybrid with good aqueous solution processability and opens the possibility of using them under complicated aqueous conditions for biorelated applications.

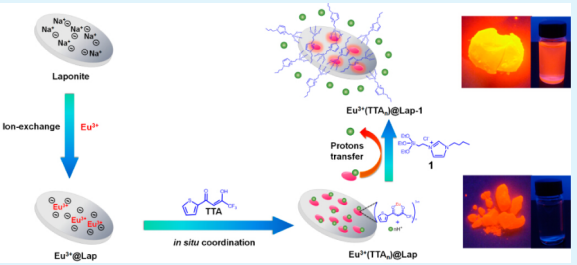

KEYWORDS: *nanohybrid, Laponite, lanthanide, luminescence, flexible film*

1. INTRODUCTION

Lanthanide-based organic−inorganic hybrid materials (LnOIH) resulting from the embedding of lanthanide complexes within inorganic matrices constitute an intensive research subject for decades, due to the great interest in them for pure academic activity and for potentially practical applications.[1−12] Recently, a luminescent molecular hybrid material, which is a viscous liquid at room temperature, has been realized by grafting Eu^{3+}-β-diketonate complex to a silicon corner of polyhedral oligomeric silsesquioxane.[13] Improvements in thermal and photostability of lanthanide complexes were attained in the resulting LnOIH.[14−16] Moreover, the fine manipulations of luminescence colors as well as the realization of white light were also achieved via the confinement of lanthanide complexes within inorganic matrices.[17−19] Despite their versatility and intriguing optical properties (such as large Stoke shifts, narrow emission bands, and long luminescence lifetimes of lanthanide ions), LnOIHs that are sufficiently bright in aqueous solution are rarely reported owing to effective radiationless deactivation of the excited state through weak coupling with the vibrational states of high-frequency OH oscillators of water ligand,[20−22] which further excludes them from biological applications such as bioimaging and biolabeling. Therefore, the development of facile and environmentally friendly methodologies to prepare LnOIH showing high luminescence efficiency in aqueous solution is highly desirable for biological applications and has still remained a challenge.

Herein we report a simple two-step strategy to fabricate nano-LnOIH exhibiting high luminescence efficiency in water. First, the in situ formation of Eu^{3+}-β-diketonate complex ($Eu^{3+}(TTA_n)$, TTA = 2-thenoyltrifluoroacetate) on surface of Laponite platelets in aqueous solution leads to luminescent nano-LnOIH. Subsequently, an imidazolium salt with reactive silane groups (**1**)[23] is loaded on surface of the platelets via ion exchange, and some of them are simultaneously covalently grafted to the edge of the platelets through adding **1** to the aqueous suspension of the nano-LnOIH and sonicating the mixture for several minutes. The modification with **1** affords the luminescent nanohybrid in aqueous environment a very high absolute quantum yield of ∼0.7, a high value that is rarely seen for LnOIH in water. A consequence is that strongly luminescent transparent material can be prepared on glass substrate and LED cell using aqueous solution of the luminescent nanohybrid. The transparent, flexible, and strongly luminescent self-standing film can also be obtained through casting aqueous solution of the luminescent nanohybrid with a small amount of water-soluble organic polymer like poly(vinyl alcohol) (PVA). The mechanism behind the high luminescence efficiency of the obtained nano-LnOIH in aqueous environment was clearly elucidated. More importantly, this approach is convenient and environmentally friendly (water is mainly used

Received: November 25, 2014
Accepted: January 5, 2015

DOI: 10.1021/am508265s
ACS Appl. Mater. Interfaces XXXX, XXX, XXX−XXX

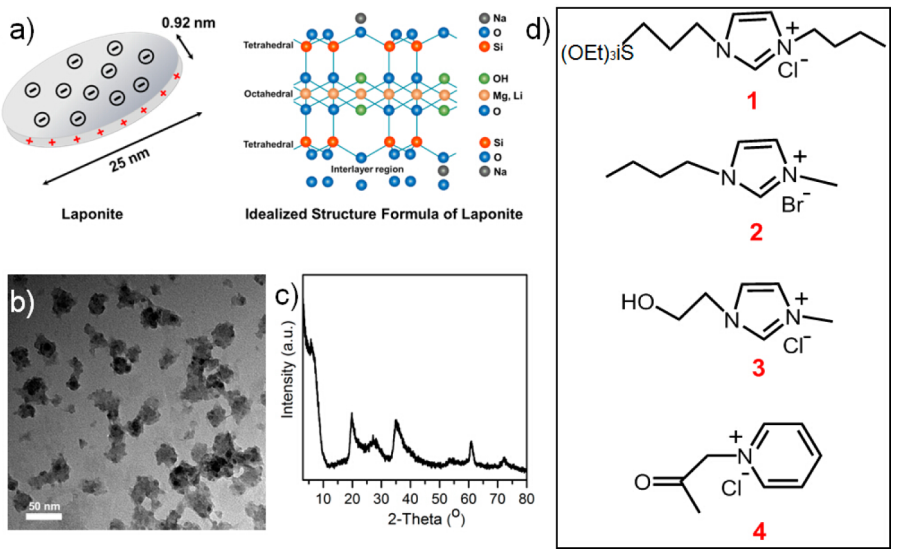

Figure 1. (a) Schematic representation of single Laponite crystal (left) and its idealized structure formula (right). (b) TEM image of Laponite platelets. (c) XRD pattern of Laponite platelets. (d) Chemical structures of the organic salts used in this study.

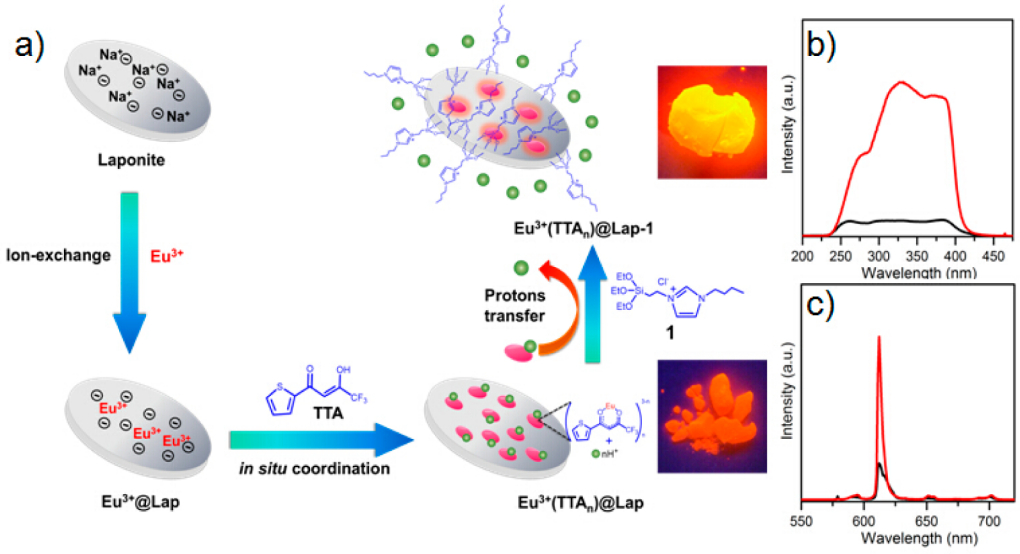

Figure 2. (a) Fabrication process of the luminescent nano-LnOIH with photographs under near UV-light illumination. For Eu^{3+}(TTAn)@Lap-**1**, the amount of **1** actually used per unit cell is 6.3. (b) Excitation spectra monitored at 612 nm and (c) emission spectra excited at 340 nm of Eu^{3+}(TTAn)@Lap (black line) and Eu^{3+}(TTAn)@Lap-**1** (red line).

as the solvent), with no need for multistep synthetic procedures, sophisticated equipment, and harsh conditions.

2. RESULTS AND DISCUSSION

Characterization of the Nanohybrid. Laponite was selected as the platform for preparing the luminescent nano-LnOIH, which is a member of the trioctahedral smectite clay family (chemical composition $Na_{0.7}[Si_8Mg_{5.5}Li_{0.3}]O_{20}(OH)_4$). Its structure, morphology, and XRD pattern is shown in Figure 1.[24−27] As synthesized nanoclay (Figure 1a), Laponite is composed of stacked platelets of an average diameter 25 nm and 0.92 nm in height, which can be completely delaminated to individual disks to form transparent solution when they are dispersed in water. Each single laponite platelet contains roughly 1500 unitary cells (u.c.). The Laponite disk surface charges negatively; both cations[25] and neutral organic molecules[28] can be readily accommodated on the individual disks, which allows for the in situ formation of Eu^{3+}-β-diketonate complexes on the disks in aqueous solution to form luminescent nano-LnOIH named as $Eu^{3+}(TTA_n)$@Lap.

$Eu^{3+}(TTA_n)$@Lap was obtained by adding TTA dissolved in minimum amount of EtOH to Eu^{3+}-containing Laponite aqueous suspension as described in Experimental Section. The experimentally determined Eu^{3+} and TTA loading per u.c. ≈ 0.3 and ∼1.1, respectively. The presence of the TTA ligand can be straightforwardly detected by UV−vis absorption spectra shown in Supporting Information, Figure S1. The bands at 265 and 340 nm in the absorption spectrum of $Eu^{3+}(TTA_n)$@Lap are assigned to the absorption of TTA ligands.[29] The formation of $Eu^{3+}(TTA_n)$ complexes on the platelets is easily seen by naked eyes under UV illumination (Figure 2a) and is well-demonstrated by excitation and emission spectrum (Figure2b,c). An appropriate amount of **1** dissolved in water was added to $Eu^{3+}(TTA_n)$@Lap, which is highly dispersed in

DOI: 10.1021/am508265s
ACS Appl. Mater. Interfaces XXXX, XXX, XXX−XXX

aqueous solution, and the mixture was sonicated for several minutes. A wet gel containing at least 80% water (determined from Thermogravimetric Analysis (TG) curves) was obtained after centrifugation, which was denoted as $Eu^{3+}(TTA_n)$@Lap-**1**. **1** can be loaded on Laponite platelets via exchanging a cation[25] and/or via grafting to the edges of the platelets through condensation of the bulky triethxoysilane moiety with the OH groups present at the edge of the platelets.[30−32] Because the platelets of Eu^{3+}(TTAn)@Lap have a low negative surface charge (zeta potential ζ = −12 mV), **1** with positive charge is strongly favored. After **1** was added into the Eu^{3+}(TTAn)@Lap, electrostatic interaction reverses the negative charge of the platelet (ζ = +23 mV).[33] However, the cointeraction or ion pair adsorption could not be excluded.[32] The presence of **1** is clearly seen from the UV−vis absorption spectra shown in Supporting Information, Figure S1. Strong band at 240 nm in Figure S1 is assigned to the absorption of imidazole ring of **1**, verifying the loading of **1** on the platelets during the modification processing. The grafting reaction is clearly evidenced in Figure 3, which

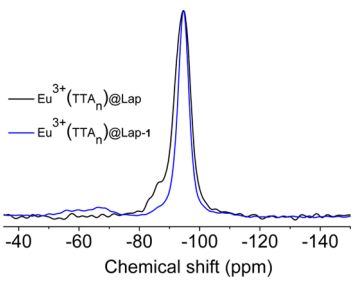

Figure 3. Solid-state ^{29}Si DP/MAS spectra of samples.

illustrates the ^{29}Si solid-state NMR spectra of the samples. The spectrum of $Eu^{3+}(TTA_n)$@Lap shows a large peak at −95 ppm assigned to the completely condensed silicon and a smaller peak with a shoulder at −85 ppm, which represents the uncondensed silicons.[34] After modification with **1**, the relative intensity of peak at −85 ppm is clearly decreasing due to the grafting reaction between **1** and the SiOH groups of Laponite sheet, and the appearance of two broad bands is observed at −67 and −56 ppm, corresponding to different condensation levels of the Si−O moieties.[30,31]

Optical Properties. $Eu^{3+}(TTA_n)$@Lap displays a pronounced increase in luminescence efficiency upon modification with **1**, as revealed by the digital photo taken under near-UV illumination (Figure 2a), excitation and emission spectra (Figure 2b,c), and the absolute quantum yield. The broad bands in the range from 200 to 420 nm exhibited in the excitation spectra are due to the absorption of TTA, which is overlapped with the absorption spectra (Figure S1). The emission spectra excited at 340 nm show five sharp lines attributed to the $^5D_0 \rightarrow {}^7F_J$ (J = 0−4) transitions. The $^5D_0 \rightarrow {}^7F_2$ transition at 612 nm dominates the emission spectra and is responsible for the bright red emission shown in Figure 2a. The absolute quantum yield determined by the integrating sphere also increases by ca. 7-fold, from 0.10 to 0.70, a high value that is rarely observed for LnOIH in aqueous solution. We are extremely surprised that Eu^{3+} exhibits so large quantum yield in the water-abundant environment since the parity-forbidden f → f transition is typically quenched in OH-containing solvents due to relaxation via O−H vibrations.[3,20] This indicates that water molecules coordinated to Eu^{3+} ions were replaced by TTA ligands after modification with **1**, which is further supported by the luminescence decay time and the intensity ratio $I(^5D_0 \rightarrow {}^7F_2)/I(^5D_0 \rightarrow {}^7F_1)$. The luminescence decay time calculated from the decay curves shown in Supporting Information, Figure S2 is remarkably increased from 0.22 to 0.72 ms after modification with **1**. The prolonged lifetime of the Eu^{3+} excited state implies a displacement of water molecules from the first coordination sphere by TTA ligands, indicating that **1** is favorable to the formation of Eu^{3+}-β-dikeonate complex with large coordination number, and thereby Eu^{3+} ions are well-protected from the water molecule quenching. The number of water molecules (n_w) in the coordination sphere of Eu^{3+} was estimated based on the emission spectra and the lifetime of the $^5D_0$ state of the Eu^{3+} ions according to the method described elsewhere.[35] The result reveals that the n_w in $Eu^{3+}(TTA_n)$@Lap and $Eu^{3+}(TTA_n)$@Lap-**1** is ∼3.1 and ∼0.2, respectively, which is in good agreement with our assumption. In addition, the ratio of the integral intensity of $I(^5D_0 \rightarrow {}^7F_2)/I(^5D_0 \rightarrow {}^7F_1)$ is often used to measure the degree of Eu^{3+} symmetry variation in different local environment. It becomes larger with increasing interaction of the Eu^{3+} with its neighbors because the site symmetry decreases.[36] The modification leads to a significant increasing in intensity ratio $I(^5D_0 \rightarrow {}^7F_2)/I(^5D_0 \rightarrow {}^7F_1)$ from 11 to 18, indicative of lower symmetry of Eu^{3+} site and a larger Eu^{3+}-ligand interaction, which implies more complete coordination of Eu^{3+} to β-diketonate. No specific crystal structure is available for the hybrid materials; however, the high intensity ratio $I(^5D_0 \rightarrow {}^7F_2)/I(^5D_0 \rightarrow {}^7F_1)$ indicates that the actual coordination polyhedron will be closer to a dodecahedron or a bicapped trigonal prism than to a square antiprism.[37] Actually, the luminescence intensity of $Eu^{3+}(TTA_n)$@Lap increases gradually with increasing amount of added **1**, which reaches

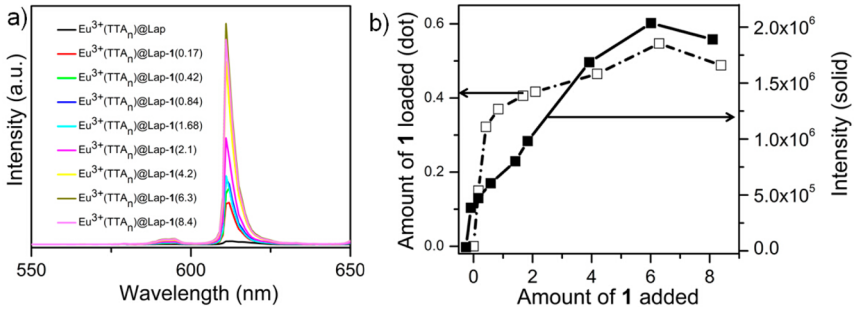

Figure 4. (a) Emission spectra of $Eu^{3+}(TTA_n)$@Lap-**1**. The excitation wavelength is 345 nm. (b) Amount of the modifier **1** loaded on the nanohybird (dot) and luminescence intensity vs the amount of **1** added to the reaction mixture (solid). The value in the brackets indicates the added amount of **1**.

DOI: 10.1021/am508265s
ACS Appl. Mater. Interfaces XXXX, XXX, XXX−XXX

its maximum when the added amount of **1** was 6.3/u.c. (Figure 4a). Interestingly, as shown in Figure 4b, all the molecules are loaded on the platelets during the modification when the added amount of **1** was low (0.17/u.c.). However, only 10% of **1** was found on the platelets if the added amount of **1** was high (6.3/u.c.).

The Mechanism for Enhancing the Luminescent Efficiency by 1. The luminescence data aforementioned reveal that the presence of **1** in luminescent nano-LnOIH can favor the formation of Eu^{3+}-β-dikeonate complex with large coordination number. The questions are why and how can **1** increase the coordination number of Eu^{3+}-β-dikeonate complex accommodated on the platelets. It has been well-documented that abundant acidic sites exist on the surface of the individual delaminated platelets of Laponite in water.[38,39] The acidic sites have negative influence on the luminescence efficiency of lanthanide complexes on the Laponite platelets.[38] TTA ligand can be protonated under the acidic environment of Laponite platelets higly dispersed in water, which competes with full coordination to Eu^{3+} ions (Scheme 1). We therefore can reason

Scheme 1. Formation of Eu^{3+}-β-Dikeonate Complex

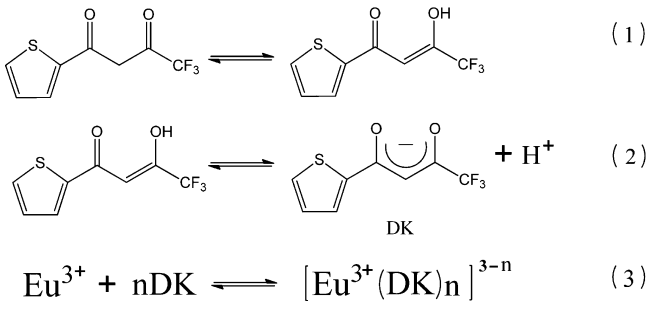

that **1** can decrease the proton activity on the platelet surface. We propose that the protons on the Laponite platelets can be removed by **1** presumably through a mechanism of synergic effect of ion exchange and neutralization. The proposed mechanisms can be further supported by the following observations: (1) the pH of an aqueous solution of **1** (2 mg mL^{-1}) was measured, and a pH of 7.9 was observed, implying **1** can act as a weak base to neutralize the protons on the platelet surfaces; and (2) the aqueous suspension of $Eu^{3+}(TTA_n)$@Lap displays a decrease in pH from ~7.3 to 6.7 even after adding a low amount (0.17/u.c.) of **1**, indicating the releasing of protons from the surface to water by exchanging H^+ with positively charged part of **1**. This can explain why a large intensity enhancement was observed after adding only a low amount of **1**, for example, 0.17/u.c. (Figure 4a). It is worth noting that other imidazolium salts (**2**−**3**) and pyridium salts showing weak acidity in aqueous solution (pH 4.2−5.8) can also be effective to enhance the luminescence of $Eu^{3+}(TTA_n)$@Lap but to a lesser extent (Figure 5). A similar luminescence-boosting effect was previously observed by us in the nanozeolite L-based luminescent nano-LnOIH; however, the mechanism responsible for decreasing the proton strength was not clearly elucidated.[40] Furthermore, the advantages of Laponite platelet over zeolites lie on its complete delamination in water and on its "soft" confinement of guests because the guest species are normally accommodated between interlayers that can to some extent adjust to the thickness of a guest species.[41]

Aqueous Solution Processability of the Nanohybrid and the Flexible Luminescent Film. The luminescent

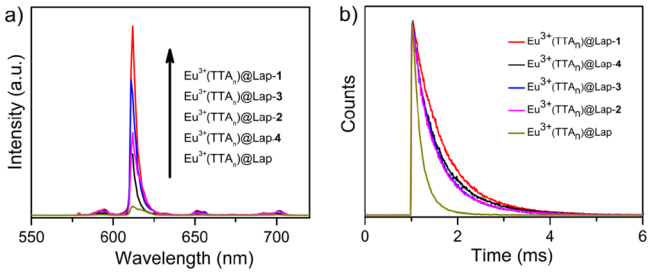

Figure 5. (a) Emission spectra at 345 nm excitation. (b) Decay curves measured at room temperature using an excitation of 345 nm and monitored around the most intense emission line at 612 nm.

boosting effect of **1** for the nanohybrid is even more significant when these nanohybrids were applied in aqueous environments. We prepared visually clear aqueous solution with $Eu^{3+}(TTA_n)$@Lap and $Eu^{3+}(TTA_n)$@Lap-**1** at a low concentration (~2 $mgmL^{-1}$); only that of the **1**-modified nano-LnOIH exhibited a bright emission under UV-light illumination (inset of Figure 6a). The $Eu^{3+}(TTA_n)$@Lap-**1** aqueous solution

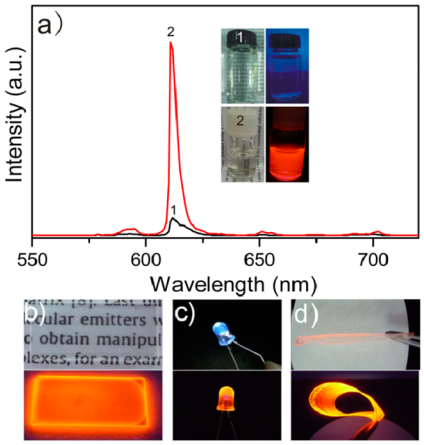

Figure 6. Demonstrations of the aqueous solution processability of the luminescent nanohybrid. (a) Emission spectra of aqueous solution of $Eu^{3+}(TTA_n)$@Lap (1) and $Eu^{3+}(TTA_n)$@Lap-**1** (2). (inset) Photographs of same under daylight (top) and UV-light irradiation (bottom). (b) A luminescent and transparent film results from casting the aqueous solution of $Eu^{3+}(TTA_n)$@Lap-**1** on a glass substrate. (c) The commercially available UV-LED (λ_{max} = 395 nm) and that coated with $Eu^{3+}(TTA_n)$@Lap-**1**. (d) The flexible film casting aqueous solution of the $Eu^{3+}(TTA_n)$@Lap-**1** with a small amount of water-soluble organic polymer like PVA.

exhibits an absolute quantum yield of 0.42 and a decay time of 0.68 ms, while the value for the aqueous solution of $Eu^{3+}(TTA_n)$@Lap is 0.05 and 0.2 ms, respectively. The success in obtaining luminescent thin film is highly desirable for a luminescent material to be fabricated into optical device; transparent film was therefore prepared by simply dropping the aqueous solution of $Eu^{3+}(TTA_n)$@Lap-**1** onto a glass substrate, followed by drying at 60 °C in air. Bright red emission under a UV-light illumination was then observed (Figure 6b). In addition to being coated on the flat substrate, the aqueous solution can be easily casted on a round-shaped objective such as an LED cell, and then a bright red light is achieved (Figure 6c).

Red-emitting luminescent materials excited effectively by near-UV light are highly desirable for white light-emitting

DOI: 10.1021/am508265s
ACS Appl. Mater. Interfaces XXXX, XXX, XXX−XXX

LED.[42] Since flexible luminescent films show great potential in collapsible optoelectronic devices owing to their advantages of foldability and crack resistance,[43] we also prepared highly luminescent and transparent flexible films using $Eu^{3+}(TTA_n)$@Lap-**1** as the building blocks via a very simple process: casting aqueous solution of the $Eu^{3+}(TTA_n)$@Lap-**1** with a small amount of water-soluble organic polymer like PVA. Very interestingly, the resultant flexible film shows bright red light even under daylight (Figure 6d, top). Strong bright red-emission light is observed when the flexible film was illuminated with a UV light (Figure 6d). The excitation and emission spectra of the flexible films shown in Figure 7 are similar to

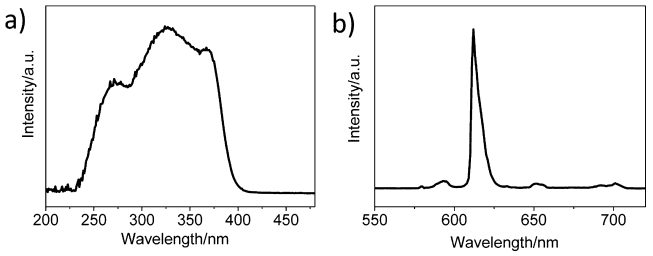

Figure 7. Excitation spectrum (a) monitored at 612 nm and emission spectrum (b) excited at 345 nm of the flexible thin film.

those displayed in Figure 2. The excitation spectrum is composed of a broad band ranging from 200 to 400 nm. It is attributed to the absorption of TTA ligand. Excitation at 345 nm leads to the same $^5D_0 \rightarrow {}^7F_J$ emission line as observed in Figures 2 and 6 with the $^5D_0 \rightarrow {}^7F_2$ band as the most prominent feature. The luminescence lifetime was determined to be 0.53 ms from the mono-exponential decay curve (Supporting Information, Figure S3). The absolute quantum yield was determined to be 0.45. The photophysical data of the film are smaller than those of the wet gel. The interaction of the luminescent nanohybrid with PVA polymer might account for the decreased luminescence efficiency. The optimization of the preparation procedure, for example, choosing an appropriate polymer, is under investigation.

3. CONCLUSION

In summary, we have demonstrated a simple and environmentally friendly way to achieve luminescent nanohybrid of sufficient brightness in water by in situ formation of Eu^{3+}-β-dikeonate complexes on aqueous dispersible nanoclay and further modification with a silane-functionalized imidazolium salt. The mechanism responsible for the surprisingly high luminescence efficiency of the nanohybrid in aqueous medium has been elucidated. The result is that the removal of the abundant protons on the Laponite platelets through a mechanism of synergic effect of ion exchange and neutralization drives the formation of Eu^{3+}-β-diketonate complexes with high coordination number. The resulting highly luminescent nano-LnOIH has also been used as building blocks for fabricating transparent film on a substrate, red-emitting LED, as well as flexible and crack resistive nano-LnOIH/polymer composite film by aqueous solution process. Our results represent a major step forward in the research on LnOIH that is highly luminescent in aqueous environment and also show great interest for applications in different fields of optoelectronics and bioimaging. Furthermore, our results highlight the importance of understanding the influence of inorganic matrices on the properties (e.g., luminescence) of lanthanide complexes in LnOIH and serve as a basis for the rational design of highly luminescent materials.[38,40]

4. EXPERIMENTAL SECTION

Materials. 2-Thenoyltrifluoroacetone (TTA), (chloropropyl)-triethoxysilane, and 1-butylimidazole were purchased from Aldrich and were used as received. Laponite RD was purchased from Rockwood Additives Ltd. and was used as received. Aqueous solutions of $EuCl_3 \cdot 6H_2O$ were prepared by dissolving Eu_2O_3 in concentrated hydrochloride acid. The imidazolium salt **1** was synthesized and characterized according to the procedure reported in ref 23.

In Situ Formation of Eu^{3+}-β-Dikeonate Complexes on Laponite Platelets. Laponite RD (0.5 g) was dispersed in deionized water (10 mL) and was sonicated for 1 h to obtain a colloidal suspension solution. A solution of 5 mL of $EuCl_3 \cdot 6H_2O$ was added to it, and then the mixture was stirred at 80 °C for 24 h. A wet gel was obtained by centrifugation. The wet gel was added into 10 mL of ethanol solution of TTA (0.15 g) and was sonicated for 2 h. The $Eu^{3+}(TTA_n)$@Lap was obtained after centrifugation.

Modification of $Eu^{3+}(TTA_n)$@Lap with 1. $Eu^{3+}(TTA_n)$@Lap wet gel (100 mg) was dispersed in 20 mL of water containing an appropriate amount x of **1**, and the mixture was sonicated for 2 h. The product was recovered by centrifugation and denoted as $Eu^{3+}(TTA_n)$@Lap-**1**(x), where x represents the number of **1** per u.c. of Laponite.

Preparation of the Transparent Film. $Eu^{3+}(TTA_n)$@Lap-**1**(6.3) (0.1 g) wet gel was dispersed in 20 mL of deionized water and was sonicated for 1 h to obtain a visually clear solution. A transparent and luminescent thin film was formed by dropping the solution on micro slide glasses, followed by evaporation of water at 60 °C in air.

Preparation of Flexible and Luminescent Films. PVA (0.2 g) was dissolved in 10 mL of water. An aqueous solution of $Eu^{3+}(TTA_n)$@Lap-**1**(6.3) was then added and sonicated for 30 min. The flexible and luminescent films were formed by dropping the mixed solution on glass, followed by evaporation of water at 60 °C in air for 10 h. The films were then peeled from the glass.

pH Measurement. Before a pH meter is used, the electrodes must be rinsed with distilled water and allowed to drain (not dried, however). They can be blotted with a paper tissue. The meter should be standardized with two buffers, one with pH below (4.00) and one with pH above (9.18) the values to be measured. The temperature of the standard buffers is measured, and the temperature compensation control is adjusted to the temperature of the solution. When the meter has been standardized and readings are stable, the pH of the test solution can be measured.

Eu^{3+}@Lap (0.1 g), Eu^{3+}(TTAn)@Lap (0.1 g), and $Eu^{3+}(TTA_n)$@Lap-**1** (0.1 g) wet gel were dispersed in 20 mL of deionized water and then were transferred to three beakers (50 mL) after sonication for 1 h. An electrode from a pH meter was then submerged into the solution that was previously prepared; the solution was allowed to stir until the pH meter gave an accurate reading. This process was repeated until the readings are almost same.

Quantification of 1 on $Eu^{3+}(TTA_n)$@Lap-1. The amount of **1** loaded on the nanohybrid was determined by measuring the absorbance at 211 nm by UV−vis spectroscopy.

Characterization. SEM images were obtained from an FE-SEM (Hitachi S-4300) at an acceleration voltage of 10 kV. The steady-state luminescence spectra and the lifetime measurements were measured on an Edinburgh Instruments FS920P near-infrared spectrometer, with a 450 W xenon lamp as the steady-state excitation source, a double excitation monochromator (1800 lines·mm^{-1}), an emission monochromator (600 lines·mm^{-1}), a semiconductor cooled Hamamatsu RMP928 photomultiplier tube. Absolute quantum yield measurements were carried on the aforementioned fluorescence spectrophotometer equipped with an integrating sphere. The fluorescence quantum yield of the sample was obtained according to the manual provided by the company. The pH of the solution was measured with a PHS-3C pH meter (Rex Instrument Factory, Shanghai, China). The zeta potential values of the micelles were determined on a Brookhaven ZetaPALS (Brookhaven Instrument, U.S.A.) at 25 °C. The instrument utilizes

DOI: 10.1021/am508265s
ACS Appl. Mater. Interfaces XXXX, XXX, XXX−XXX

phase analysis light scattering to provide an average over multiple particles. Doubly distilled water was used as the background electrolyte for zeta potential measurements. A UV−visible Agilent cray100 spectrometer, with a quartz cuvette with path length 10 mm, was used to determine the wavelength of the maximum UV absorbance peak. The absorbance was measured from 200 to 800 nm.

■ ASSOCIATED CONTENT

Ⓢ Supporting Information

UV−vis absorption spectra of $Eu^{3+}(TTA_n)$@Lap and $Eu^{3+}(TTA_n)$@Lap-**1** in water, luminescence decay curves of $Eu^{3+}(TTA_n)$@Lap and $Eu^{3+}(TTA_n)$@Lap-**1** measured at room temperature, luminescence decay curves of the flexible thin film. This material is available free of charge via the Internet at http://pubs.acs.org.

■ AUTHOR INFORMATION

Corresponding Author

*Phone: 86-22-60203674. Fax: 86-22-60204294. E-mail: lihuanrong@hebut.edu.cn.

Notes

The authors declare no competing financial interest.

■ ACKNOWLEDGMENTS

Financial support by the National Natural Science Foundation of China (21171046, 21271060, and 21236001), the Tianjin Natural Science Foundation (13JCYBJC18400), the Natural Science Foundation of Hebei Province (No. B2013202243), and Educational Committee of Hebei Province (2011141, LJRC021) is gratefully acknowledged.

■ REFERENCES

(1) Carlos, L. D.; Ferreira, R. A. S.; Bermudez, V. D.; Ribeiro, S. J. L. Lanthanide-Containing Light-Emitting Organic-Inorganic Hybrids: A Bet on the Future. *Adv. Mater.* **2009**, *21*, 509−534.

(2) Eliseeva, S. V.; Bunzli, J. C. G. Lanthanide luminescence for Functional Materials and Bio-Sciences. *Chem. Soc. Rev.* **2010**, *39*, 189−227.

(3) Binnemans, K. Lanthanide-Based Luminescent Hybrid Materials. *Chem. Rev.* **2009**, *109*, 4283−4374.

(4) Feng, J.; Zhang, H. J. Hybrid Materials Based on Lanthanide Organic Complexes: a review. *Chem. Soc. Rev.* **2013**, *42*, 387−410.

(5) Carlos, L. D.; Ferreira, R. A. S.; Bermudez, V. D.; Julian-Lopez, B.; Escribano, P. Progress on Lanthanide-Based Organic-Inorganic Hybrid Phosphors. *Chem. Soc.Rev.* **2011**, *40*, 536−549.

(6) Yan, B. Recent Progress in Photofunctional Lanthanide Hybrid Materials. *RSC. Adv.* **2012**, *2*, 9304−9324.

(7) Sendor, D.; Kynast, U. Efficient Red-Emitting Hybrid Materials Based on Zeolites. *Adv. Mater.* **2002**, *14*, 1570−1574.

(8) Wang, Y.; Li, H. R.; Feng, Y.; Zhang, H. J.; Calzaferri, G.; Ren, T. Z. Orienting Zeolite L Microcrystals with a Functional Linker. *Angew. Chem., Int. Ed.* **2010**, *49*, 1434−1438.

(9) Lezhnina, M.; Benavente, E.; Bentlage, M.; Echevarria, Y.; Klumpp, E.; Kynast, U. Luminescent Hybrid Material Based on a Clay Mineral. *Chem. Mater.* **2007**, *19*, 1098−1102.

(10) Monguzzi, A.; Macchi, G.; Meinardi, F.; Tubino, R.; Burger, M.; Calzaferri, G. Sensitized near Infrared Emission from Lanthanide-Exchanged Zeolites. *Appl. Phys. Lett.* **2008**, *92*, 123301.

(11) Xu, J.; Jia, L.; Jin, N. Z.; Ma, Y. F.; Liu, X.; Wu, W. Y.; Liu, W. S.; Tang, Y.; Zhou, F. Fixed-Component Lanthanide-Hybrid-Fabricated Full-Color Photoluminescent Films as Vapoluminescent Sensors. *Chem.—Eur. J.* **2013**, *19*, 4556−4562.

(12) Meyer, L. V.; Schonfeld, F.; Muller-Buschbaum, K. Lanthanide Based Tuning of Luminescence in MOFs and Dense Frameworks - from Mono- and Multimetal Systems to Sensors and Films. *Chem. Commun.* **2014**, *50*, 8093−8108.

(13) Chen, X. F.; Zhang, P. N.; Wang, T. R.; Li, H. R. The First Europium(III) *β*- Diketonate Complex Functionalized Polyhedral Oligomeric Silsesquioxane. *Chem.—Eur. J.* **2014**, *20*, 2551−2556.

(14) Fernandes, M.; Bermudez, V. D.; Ferreira, R. A. S.; Carlos, L. D.; Charas, A.; Morgado, J.; Silva, M. M.; Smith, M. J. Highly Photostable Luminescent Poly(Epsilon-Caprolactone)Siloxane Biohybrids Doped with Europium Complexes. *Chem. Mater.* **2007**, *19*, 3892−3901.

(15) Wang, Y. G.; Li, H. R.; Gu, L. J.; Gan, Q. Y.; Li, Y. N.; Calzaferri, G. Thermally Stable Luminescent Lanthanide Complexes in Zeolite L. *Microporous Mesoporous Mater.* **2009**, *121*, 1−6.

(16) Ding, Y. X.; Wang, Y. G.; Li, H. R.; Duan, Z. Y.; Zhang, H. H.; Zheng, Y. X. Photostable and Efficient Red-Emitters Based on Zeolite L Crystals. *J. Mater. Chem.* **2011**, *21*, 14755−14759.

(17) Wada, Y.; Sato, M.; Tsukahara, Y. Fine Control of Red-Green-Blue Photoluminescence in Zeolites Incorporated with Rare-Earth Ions and a Photosensitizer. *Angew. Chem., Int. Ed.* **2006**, *45*, 1925−1928.

(18) Zhao, D.; Seo, S. J.; Bae, B. S. Full-Color Mesophase Silicate Thin Film Phosphors Incorporated with Rare Earth Ions and Photosensitizers. *Adv. Mater.* **2007**, *19*, 3473−3479.

(19) Wang, T. R.; Li, P.; Li, H. R. Color-Tunable Luminescence of Organoclay-Based Hybrid Materials Showing Potential Applications in White LED and Thermosensors. *ACS Appl. Mater. Interfaces* **2014**, *6*, 12915−12921.

(20) Zhang, J.; Liu, Y.; Li, Y.; Zhao, H. X.; Wan, X. H. Hybrid Assemblies of Eu-Containing Polyoxometalates and Hydrophilic Block Copolymers with Enhanced Emission in Aqueous Solution. *Angew. Chem., Int. Ed.* **2012**, *51*, 4598−4602.

(21) Diniz, J. R.; Correa, J. R.; Moreira, D. d. A.; Fontenele, R. S.; de Oliveira, A. L.; Abdelnur, P. V.; Dutra, J. D. L.; Freire, R. O.; Rodrigues, M. O.; Neto, B. A. D. Water-Soluble Tb^{3+} and Eu^{3+} Complexes with Ionophilic (Ionically Tagged) Ligands as Fluorescence Imaging Probes. *Inorg. Chem.* **2013**, *52*, 10199−10205.

(22) De Bettencourt-Dias, A.; Barber, P. S.; Bauer, S. A. Water-Soluble Pybox Derivative and Its Highly Luminescent Lanthanide Ion Complexes. *J. Am. Chem. Soc.* **2012**, *134*, 6987−6994.

(23) Lu, Y.; Moganty, S. S.; Schaefer, J. L.; Archer, L. A. Ionic liquid-Nanoparticle Hybrid Electrolytes. *J. Mater. Chem.* **2012**, *22*, 4066−4072.

(24) Lezhnina, M. M.; Grewe, T.; Stoehr, H.; Kynast, U. Laponite Blue: Dissolving the Insoluble. *Angew. Chem., Int. Ed.* **2012**, *51*, 10652−10655.

(25) Lotsch, B. V.; Ozin, G. A. Clay Bragg Stack Optical Sensors. *Adv. Mater.* **2008**, *20*, 4079−4084.

(26) LeBaron, P. C.; Wang, Z.; Pinnavaia, T. J. Polymer-Layered Silicate Nanocomposites: an overview. *Appl. Clay. Sci.* **1999**, *15*, 11−29.

(27) Dawson, J. I.; Oreffo, R. O. C. Clay: New Opportunities for Tissue Regeneration and Biomaterial Design. *Adv. Mater.* **2013**, *25*, 4069−4086.

(28) Felbeck, T.; Behnke, T.; Hoffmann, K.; Grabolle, M.; Lezhnina, M. M.; Kynast, U. H.; Resch-Genger, U. Nile-Red-Nanoclay Hybrids: Red Emissive Optical Probes for Use in Aqueous Dispersion. *Langmuir* **2013**, *29*, 11489−97.

(29) Ding, Y. X.; Wang, Y. G.; Li, H. R.; Duan, Z. Y.; Zhang, H. H.; Zheng, Y. X. Photostable and Efficient Red-Emitters Based on Zeolite L Crystals. *J. Mater. Chem.* **2011**, *21*, 14755−14759.

(30) Herrera, N. N.; Letoffe, J. M.; Reymond, J. P.; Bourgeat-Lami, E. Silylation of Laponite Clay Particles with Monofunctional and Trifunctional Vinyl Alkoxysilanes. *J. Mater. Chem.* **2005**, *15*, 863−871.

(31) Herrera, N. N.; Letoffe, J. M.; Putaux, J. L.; David, L.; Bourgeat-Lami, E. Aqueous Dispersions of Silane-Functionalized Laponite Clay Platelets. A First Step Toward the Elaboration of Water-Based Polymer/clay nanocomposites. *Langmuir* **2004**, *20*, 1564−1571.

(32) Lotsch, B. V.; Ozin, G. A. Photonic Clays: A New Family of Functional 1D Photonic Crystals. *ACS Nano* **2008**, *2*, 2065−2074.

(33) Guerrero-Martínez, A.; Fibikar, S.; Pastoriza-Santos, I.; Liz-Marzán, L. M.; De Cola, L. Microcontainers with Fluorescent

DOI: 10.1021/am508265s
ACS Appl. Mater. Interfaces XXXX, XXX, XXX−XXX

Anisotropic Zeolite L Cores and Isotropic Silica Shells. *Angew. Chem.* **2009**, *121*, 1292−1296.
(34) Wheeler, P. A.; Wang, J. Z.; Baker, J.; Mathias, L. J. Synthesis and Characterization of Covalently Functionalized Laponite Clay. *Chem. Mater.* **2005**, *17*, 3012−3018.
(35) Fernandes, M.; de Zea Bermudez, V.; Sá Ferreira, R.; Carlos, L.; Charas, A.; Morgado, J.; Silva, M. M.; Smith, M. J. Highly Photostable Luminescent Poly (ε-Caprolactone) Siloxane Biohybrids Doped with Europium Complexes. *Chem. Mater.* **2007**, *19*, 3892−3901.
(36) Tang, S.; Babai, A.; Mudring, A. V. Europium-Based Ionic Liquids as Luminescent Soft Materials. *Angew. Chem., Int. Ed.* **2008**, *47*, 7631−7634.
(37) Lunstroot, K.; Driesen, K.; Nockemann, P.; Görller-Walrand, C.; Binnemans, K.; Bellayer, S.; Le Bideau, J.; Vioux, A. Luminescent Ionogels Based on Europium-Doped Ionic Liquids Confined within Silica-Derived Networks. *Chem. Mater.* **2006**, *18*, 5711−5715.
(38) Lezhnina, M. M.; Bentlage, M.; Kynast, U. H. Nanoclays: Two-Dimensional Shuttles for Rare Earth Complexes in Aqueous Solution. *Opt. Mater.* **2011**, *33*, 1471−1475.
(39) Auerbach, S. M.; Carrado, K. A.; Dutta, P. K. *Handbook of Layered Materials;* CRC Press: New York, 2004.
(40) Li, P.; Wang, Y. G.; Li, H. R.; Calzaferri, G. Luminescence Enhancement after Adding Stoppers to Europium(III) Nanozeolite L. *Angew. Chem., Int. Ed.* **2014**, *53*, 2904−2909.
(41) Lezhnina, M. M.; Kynast, U. H. Optical Properties of Matrix Confined Species. *Opt. Mater.* **2010**, *33*, 4−13.
(42) Li, H. F.; Zhao, R.; Jia, Y. L.; Sun, W. Z.; Fu, J. P.; Jiang, L. H.; Zhang, S.; Pang, R.; Li, C. Y. $Sr_{1.7}Zn_{0.3}CeO_4$:Eu^{3+} Novel Red-Emitting Phosphors: Synthesis and Photoluminescence Properties. *ACS Appl. Mater. Interfaces* **2014**, *6*, 3163−3169.
(43) Liang, R. Z.; Yan, D. P.; Tian, R.; Yu, X. J.; Shi, W. Y.; Li, C. Y.; Wei, M.; Evans, D. G.; Duan, X. Quantum Dots-Based Flexible Films and Their Application as the Phosphor in White Light-Emitting Diodes. *Chem. Mater.* **2014**, *26*, 2595−2600.

DOI: 10.1021/am508265s
ACS Appl. Mater. Interfaces XXXX, XXX, XXX−XXX